Near-field Raman imaging using optically trapped dielectric microsphere

Johnson Kasim,[1,2] Yu Ting,[1] You Yu Meng,[1] Liu Jin Ping,[2] Alex See,[2] Li Lain Jong,[3] and Shen Ze Xiang[1,*]

[1]*Division of Physics and Applied Physics, School of Physical and Mathematical Sciences, Nanyang Technological University, 1 Nanyang Walk, Blk 5 Level 3, Singapore 637371*
[2]*Chartered Semiconductor Manufacturing Ltd., 60 Woodlands Industrial Park D, Street 2, Singapore 738406*
[3]*School of Materials Science Engineering, Nanyang Technological University, 50 Nanyang Avenue, Singapore 637819*
[*]*Corresponding author: zexiang@ntu.edu.sg*

Abstract: The stumbling block of employing Raman imaging in nanoscience and nanotechnology is the diffraction-limited spatial resolution. Several approaches have been employed to improve the spatial resolution, among which aperture and apertureless near-field Raman techniques are the most frequently used. In this letter, we report a new approach in doing near-field Raman imaging with spatial resolution of about 80 nm, by trapping and scanning a polystyrene microsphere over the sample surface in water. We have used this technique to resolve PMOS transistors with SiGe source drain stressors with poly-Si gates, as well as gold nanopatterns with excellent reproducibility.

OCIS codes: (350.4855) Optical tweezers or optical manipulation; (170.5660) Raman spectroscopy; (170.5810) Scanning microscopy.

References and links

1. D. W. Pohl, W. Denk, and M. Lanz, "Optical stethoscopy: Image recording with resolution l/20," Appl. Phys. Lett. **44**, 651 - 653 (1984).
2. B. Hecht, H. Heinzelmann, and D. W. Pohl, "Combined aperture SNOM/PSTM: best of both worlds?," Ultramicroscopy **57**, 228 - 234 (1995).
3. J. Kim, J. H. Kim, K. B. Song, S. Q. Lee, E. K. Kim, S. E. Choi, Y. Lee, and K. H. Park, "Near-field imaging of surface plasmon on Au nano-dots fabricated by scanning probe lithography," J. Microsc. **209**, 236 - 239 (2003)
4. F. Zenhausern, Y. Martin, and H. K. Wickramasinghe, "Scanning interferometric apertureless microscopy: Optical imaging at 10 Angstrom resolution," Science **269**, 1083 - 1085 (1995).
5. D. H. Pan, N. Klymyshyn, D. H. Hu, and H. P. Lu, "Tip-enhanced near-field Raman spectroscopy probing single dye-sensitized TiO_2 nanoparticles," Appl. Phys. Lett. **88**, 093121 (2006).
6. H. G. Frey, C. Bolwien, A. Brandenburg, R. Ros, and D. Anselmetti, "Optimized apertureless optical near-field probes with 15 nm optical resolution," Nanotechnology **17**, 3105 - 3110 (2006).
7. D. P. Tsai, A. Othonos, M. Moskovits, and D. Uttamchandani, "Raman spectroscopy using a fiber optic probe with subwavelength aperture,"Appl. Phys. Lett. **64**, 1768 - 1770 (1994).
8. C. L. Jahncke, M. A. Paesler, and H. D. Hallen, "Raman imaging with near-field scanning optical microscopy," Appl. Phys. Lett. **67**, 2483 - 2485 (1995).
9. J. Grausem, B. Humbert, M. Spajer, D. Courjon, A. Burneau, and J. Oswalt, "Near-field Raman spectroscopy," J. Raman Specstrosc. **30**, 833 - 840 (1999).
10. B. Hecht, B. Sick, U. P. Wild, V. Deckert, R. Zenobi, O. J. F. Martin, and D. W. Pohl, "Scanning near-field optical microscopy with aperture probes: Fundamentals and applications," J. Chem. Phys. **112**, 7761 - 7774 (2000).
11. M. S. Anderson, "Locally enhanced Raman spectroscopy with an atomic force microscope," Appl. Phys. Lett. **76**, 3130 – 3132 (2000).
12. W. X. Sun and Z. X. Shen, "Near-field scanning Raman microscopy using apertureless probes," J. Raman Spectrosc. **34**, 668 - 676 (2003).
13. N. Anderson, A. Hartschuh, and L. Novotny, "Near-field Raman microscopy," Materials Today **May**, 50 - 54 (2005).
14. Y. Saito, M. Motohashi, N. Hayazawa, M. Iyoki, and S. Kawata, "Nanoscale characterization of strained silicon by tip-enhanced Raman spectroscope in reflection mode," Appl. Phys. Lett. **88**, 143109 (2006).
15. N. Anderson, A. Bouhelier, and L. Novotny, "Near-field photonics: tip-enhanced microscopy and spectroscopy on the nanoscale," J. Opt. A **8**, S227 – S233 (2006).

#92247 - $15.00 USD Received 29 Jan 2008; revised 2 Mar 2008; accepted 25 Mar 2008; published 19 May 2008

16. D. Richards, R. G. Milner, F. Huang, and F. Festy, "Tip-enhanced Raman microscopy: practicalities and limitations," J. Raman Spectrosc. **34**, 663 - 667 (2003).
17. N. Lee, R. D. Hartschuh, D. Mehtani, A. Kisliuk, J. F. Maguire, M. Green, M. D. Foster, and A. P. Sokolov, "High constrast scanning nano-Raman spectroscopy of silicon," J. Raman Spectrosc. **38**, 789 - 796 (2007).
18. R. Ossikovski, Q. Nguyen, and G. Picardi, "Simple model for the polarization effects in tip-enhanced Raman spectroscopy," Phys. Rev. B **75**, 045412 (2007).
19. N. Hayazawa, M. Motohashi, Y. Saito, H. Ishitobi, A. Ono, T. Ichimura, P. Verma, and S. Kawata, "Visualization of localized strain of a crystalline thin layer at the nanoscale by tip-enhanced Raman spectroscopy and microscopy," J. Raman Spectrosc. **38**, 684 - 696 (2007).
20. N. Lee, R. D. Hartschuh, D. Mehtani, A. Kisliuk, J. F. Maguire, M. Green, M. D. Foster, and A. P. Sokolov, "High constrast scanning nano-Raman spectroscopy of silicon," J. Raman Spectrosc. **38**, 789 - 796 (2007).
21. S. H. Christiansen, M. Becker, S. Fahlbusch, J. Michler, V. Sivakov, G. Andra, and R. Geiger, "Signal enhancement in nano-Raman spectroscopy by gold caps on silicon nanowires obtained by vapour-liquid-solid growth," Nanotechnology **18**, 035503 (2007).
22. M. Becker, V. Sivakov, G. Andra, R. Geiger, J. Schreiber, S. Hoffmann, J. Michler, A. P. Milenin, P. Werner, and S. H. Christiansen, "The SERS and TERS effects obtained by gold droplets on top of Si nanowires," Nano Lett. **7**, 75 - 80 (2007).
23. A. Ashkin, "Applications of laser radiation pressure," Science **210**, 1081 - 1088 (1980).
24. A. Ashkin, "Optical trapping and manipulation of neutral particles using lasers," Proc. Natl. Acad. Sci. USA **94**, 4853 - 4860 (1997).
25. X. Li, Z. G. Chen, A. Taflove, and V. Backman, "Optical analysis of nanoparticles via enhanced backscattering facilitated by 3-D photonic nanojets," Opt. Express **13**, 526 - 533 (2005).
26. S. Lecler, Y. Takakura, and P. Meyrueis, "Properties of a three-dimensional photonic jet," Opt. Lett. **30**, 2641 - 2643 (2005).
27. A. L. Birkbeck, S. Zlatanovic, S. C. Esener, and M. Ozkan, "Laser-tweezer-controlled solid immersion microscopy in microfluidic systems," Opt. Lett. **30**, 2712 - 2714 (2005).
28. K. J. Yi, H. Wang, Y. F. Lu, and Z. Y. Yang, "Enhanced Raman scattering by self-assembled silica spherical microparticles," J. Appl. Phys. **101**, 063528 (2007).
29. G. Veshapidze, M. L. Trachy, M. H. Shah, and B. D. DePaola, "Reducing the uncertainty in laser beam size measurement with a scanning edge method," Appl. Opt. **45**, 8197 - 8199 (2006).
30. E. Bonera, M. Fanciulli, and D. N. Batchelder, "Raman spectroscopy for a micrometric and tensorial analysis of stress in silicon," Appl. Phys. Lett. **81**, 3377 - 3379 (2002).
31. E. Bonera, M. Fanciulli, and D. N. Batchelder, "Combining high resolution and tensorial analysis in Raman stress measurements of silicon," J. Appl. Phys. **94**, 2729 - 2740 (2003).
32. P. R. Chidambaram, C. Bowen, S. Chakravarthi, C. Machala, and R. Wise, "Fundamentals of silicon material properties for successful exploitation of strain engineering in modern CMOS manufacturing," IEEE Trans. Electron Dev. **53**, 944 - 964 (2006).
33. D. J. Paul, "Si/SiGe heterostructures: from material and physics to devices and circuits," Semicond. Sci. Technol. **19**, R75 – R108 (2004).
34. S. L. Wu, Y. M. Lin, S. J. Chang, S. C. Lu, P. S. Chen, and C. W. Liu, "Enhanced CMOS performances using substrate strained-SiGe and mechanical strained-Si technology," IEEE Electron Device Lett. **27**, 46 - 48 (2006).
35. I. D. Wolf, H. E. Maes, and S. K. Jones, "Stress measurements in silicon devices through Raman spectroscopy: Bridging the gap between theory and experiment," J. Appl. Phys. **79**, 7148 - 7156 (1996).
36. S. Nakashima, T. Yamamoto, A. Ogura, K. Uejima, and T. Yamamoto, "Characterization of Si/Ge_xSi_{1-x} structures by micro-Raman imaging," Appl. Phys. Lett. **84**, 2533 - 2535 (2004).
37. T. Mitani, S. Nakashima, H. Okumura, and A. Ogura, "Depth profiling of strain and defects in Si/$Si_{1-x}Ge_x$/Si heterostructures by micro-Raman imaging," J. Appl. Phys. **100**, 073511 (2006).
38. E. Anastassakis and E. Liarokapis, "Polycrystalline Si under strain: Elastic and lattice-dynamical considerations,"J. Appl. Phys. **62**, 3346 - 3352 (1987).
39. V. Senez, A. Armigliato, I. D. Wolf, G. Carnevale, R. Balboni, S. Frabboni, and A. Benedetti, "Strain determination in silicon microstructures by combined convergent beam electron diffraction, process simulation, and micro-Raman spectroscopy," J. Appl. Phys. **94**, 5574 - 5583 (2003).
40. H. H. Liu, X. F. Duan, X. Y. Qi, Q. X. Xu, H. O. Li, and H. Qian, "Nanoscale strain analysis of strained-Si metal-oxide-semiconductor field effect transistors by large angle convergent-beam electron diffraction," Appl. Phys. Lett. **88**, 263513 (2006).

1. Introduction

Raman spectroscopy measures molecular vibrations, which are determined by the structure and chemical bonding as well as the masses of the constituent atoms/ions. Raman spectra are unique in chemical and structural identifications. Conventional micro-Raman spectroscopy has a spatial resolution of about 500 nm, governed by the diffraction limit. To extend Raman imaging to the study of nano-materials, extensive efforts have been made to reduce the laser spot size below the diffraction limit by using scanning near-field optical microscopy (SNOM),

#92247 - $15.00 USD Received 29 Jan 2008; revised 2 Mar 2008; accepted 25 Mar 2008; published 19 May 2008

which can be broadly divided into two approaches, laser delivered through an aperture [1–3] and tip-enhanced (apertureless) [4-6] near-field techniques.

Conventional near-field scanning Raman microscopy is based on the principle of aperture SNOM: an optical fiber with a small aperture (50 – 100 nm) is used to deliver the laser light and the fiber is kept at a close distance (~tens of nanometer) above the sample surface [7-10]. However the technique has been plagued by the very low throughput of the laser through metal-coated optical fibers (typically 100 nW) and the intrinsic weakness of the Raman scattering. A Raman mapping of modest S/N ratio takes very long time (e.g. ~10 hours). This approach has been largely abandoned for Raman imaging by researchers now. An alternative approach is to use apertureless technique, also known as tip-enhanced Raman scattering (TERS), in which laser spot focused on the tip apex creates a strongly confined optical field [11-14]. TERS is the preferred choice for performing near-field Raman scattering and 10 nm spatial resolution has been achieved [15]. However, TERS also has its severe limitations. The success of TERS experiments depends on the reproducibility of fabricating a "hot" tip, where strongly enhanced electromagnetic field can be excited on the apex of the tip. The reproducibility of this "hot" tip is still poor, due to the mismatch between the frequency of the excitation laser and the resonance frequency of the tip [16]. Due to the diffraction limit, the laser spot focused on the tip apex also causes an intense background (far-field signal) that should be eliminated to achieve better S/N ratio [17]. TERS also faces wear-tear and oxidation problems. These shortcomings must be overcome for TERS to be used for large-scale applications in nano-science and nano-technology. Recently, in order to improve the near-field Raman signal, the polarization effects have been studied to minimize the far-field signal in TERS from Si-based sample [18-20]. Another promising approach in controlling the geometry of the tip is by using nanowire. Si nanowire with gold cap was shown to be a good candidate to achieve controllable and reproducible "hot" tip for successful TERS experiments [21,22].

We have developed a new approach, which we believe is a disruptive approach to near-field Raman microscopy. In this method, the laser is focused to a spot smaller than diffraction limit by a dielectric microsphere. Besides being used as the excitation source for Raman spectroscopy, the incident laser beam is also used to hold the microsphere just above the sample surface, through the well-known optical tweezers mechanism [23,24]. Simulation studies on optical nanojet based on plane wave incident light have shown that sub-diffraction limited focusing can be achieved when the diameter of the dielectric microsphere is comparable to the wavelength of laser [25,26]. Optical tweezers controlled 10 μm solid immersion lens (SIL) was used by A. L. Birkbeck *et al.* to perform optical microscopy on chrome grating [27]. Here we show the capability of trapping a dielectric microsphere to achieve high-resolution Raman imaging. This technique has many advantages over the previous near-field techniques. The Raman signal collected with microsphere using our technique is always much stronger than that without microsphere, by 2-7 times depending on the diameter of microsphere used [28]. This is a critical advantage over the aperture near-field technique. As the laser light is focused on the sample through the microsphere, there is no far-field signal in our setup, which has been one of the limitations in TERS. There is also no requirement to use a metal or metal-coated probe, e.g. metal-coated AFM tip, to perform the experiment. The strong near-field Raman signal and the simplicity in carrying out the experiment make this technique attractive, easy and fast. The reproducibility is also excellent, close to the 100% level. We also show that this technique can also work on different types of samples.

#92247 - $15.00 USD Received 29 Jan 2008; revised 2 Mar 2008; accepted 25 Mar 2008; published 19 May 2008

2. Experimental

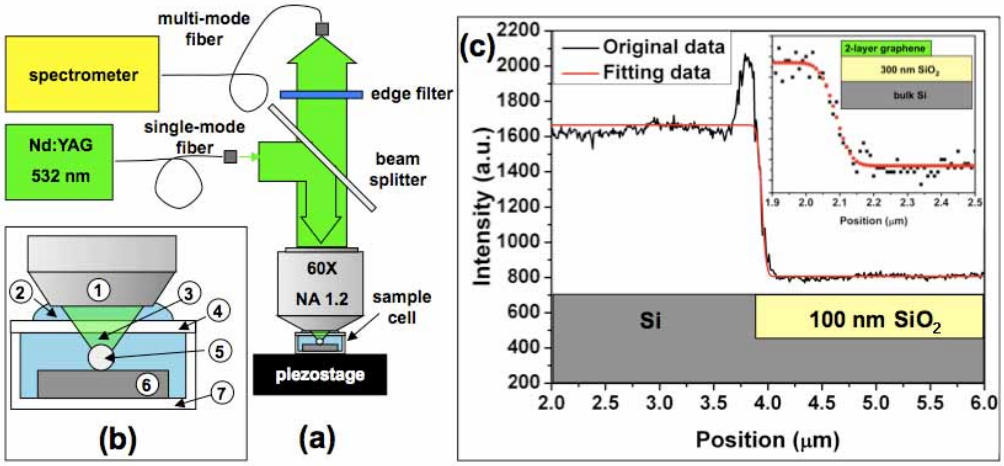

Fig. 1. (a). Schematic diagram of the near-field Raman microscope with microsphere. (b) Detailed description of the sample cell: (1) water immersion lens (60X NA=1.2 WATER IMMERSION), (2) water, (3) focused laser, (4) cover glass, (5) polystyrene microsphere (3 mm), (6) sample, and (7) sample cell. (c) Typical Si-Si Raman intensity vs position with the best fit to equation 1 to determine the laser spot size. The spot size of the beam - the full width at half maximum (FWHM), was calculated to be 78 nm. Inset shows the integrated G-band intensity vs position of a 2-layer graphene sheet. The calculated spot size is 84 nm.

The near-field Raman microscopy setup with polystyrene microsphere is based on the WITec CRM200 confocal Raman microscopy system (25 μm pinhole) with OLYMPUS microscope objective (60X NA=1.2 WATER IMMERSION), as shown in Fig. 1(a). A double-frequency Nd:YAG laser (532 nm, CNI Laser) is used as the excitation laser. The laser is coupled into a 3.5 μm-core diameter single mode fiber. The linearly polarized Gaussian beam (TEM_{00}) used to excite the Raman signal is also used to trap the microsphere. A linear attenuator was used to reduce the laser power on the sample, which was about 3 mW. The laser beam is incident on the sample through the microsphere. Sample is placed in a sample cell with diluted polystyrene microspheres (diameter = 3 μm) in de-ionized water. One microsphere was trapped at the center of the laser beam laterally by the gradient force arising from the gradient in light intensity, and was pushed down by the scattering force to the sample surface[24]; hence the microsphere was in contact with the surface of the sample during scanning. The sample cell is put on a translation stage, which can be moved coarsely along *x*- and *y-axes*. It also can be finely moved with a piezostage. The piezostage has 100 μm of travel distance along *x*- and *y*-directions and 20 μm in the *z*-direction. The Raman scattered light was directed to either 1800 grooves/mm or 600 grooves/mm grating and detected using a TE-cooled charge-coupled-device (CCD) cooled to -64 ^{o}C. The spectral resolution is 1 cm^{-1}, read directly from the spectrometer and after curve fitting the spectral difference of 0.02 cm^{-1} can be resolved. The stage movement and data acquisition were controlled using ScanCtrl Spectroscopy Plus software from WITec GmbH, Germany. Fitting of single spectrum was done using Renishaw WiRE2.0 software. Data analysis for Raman images was done using WITec Project software. Polystyrene microspheres were purchased from Polysciences, Inc. Scanning electron micrographs were taken with Field Emission SEM (JEOL JSM-6700F), set to 10 keV.

3. Results and discussion

The laser spot size of our near-field Raman technique was determined by using a scanning-edge method [29]. Before scanning, real-time observation of the peak intensity was done to ensure the focus was on the sample surface. The trapped microsphere was scanned across

#92247 - $15.00 USD Received 29 Jan 2008; revised 2 Mar 2008; accepted 25 Mar 2008; published 19 May 2008

Si/SiO_2 structure with 10 nm step size and the Si intensity spectrum (Fig. 1(c)) was fitted with the Eq. (1),

$$I(x) = \frac{P}{2}\left\{1 - erf\left(\frac{\sqrt{2}(x - x_o)}{w}\right)\right\} \quad (1)$$

where P is the total power contained in the laser beam, x is the position of the scanning edge, x_0 is the center of the beam and w is the $1/e^2$ half-width. The spot size of the beam - the full width at half maximum (FWHM), was calculated to be 78 nm from the following relationship, $FWHM = \sqrt{2\ln 2}w$. Note that there is a sudden increase of Si intensity at the edge of the trench. This can be attributed to a change in polarization of the light in the focal volume, which may be induced by inhomogeneities of the surface, changing the Raman selection rules as pointed as in the experiments done by E. Bonera *et al* [30,31]. To eliminate the uncertainty caused by the edge effect, we have also scanned the edge of a very thin 2-layer graphene sheet on SiO_2/Si substrate and the spot size was 84 nm (inset of Fig. 1(c)). Our experimental spot size is smaller than the simulation results (120 nm) based on plane wave incident light [28]. This may be due to the tight focus light and also the interaction of the light with the substrate. At this point, simulation studies are still being carried out to further understand the mechanism of this approach.

In this paper, we focus on the study of PMOS transistors with SiGe source drain stressors and poly-Si gate. The patterned wafers used in this study were prepared using 65 nm device technology. After spacer formation and Si recess etch, the wafers were cleaned and the epitaxial SiGe growth was performed on a commercially available low-pressure chemical vapor deposition (LPCVD) system. We also show the capability of our technique in studying the strain on the channel below the poly-Si gates, which is compressively strained by the SiGe stressors.

Straining the silicon can suppress the inter-valley scattering and reduce the effective carrier mass. Hence, it results in an improvement of the effective carrier mobility in the Si channel. Semiconductor industry has used mechanical strain as an alternative to physical scaling in improving the transistor performance [32]. Appropriate strain applied to the channel region can significantly improve transistor performance. However, in complementary metal-oxide-semiconductor (CMOS) transistor, n-MOS and p-MOS need to be strained differently. The compressive strain is known to be beneficial for p-MOS and the tensile strain is known to improve the n-MOS performance [33,34]. That is why a technique to characterize strain with sub-100 nm resolution reliably is high in demand.

Micro-Raman spectroscopy has been a popular tool for strain measurements because it is non-destructive and quantitative [35-37]. Compressive strain shifts the Raman peak to higher frequency, while the tensile strain result in a red shift [38]. However, the spatial resolution of micro-Raman makes it impossible to be used for strain characterization in sub-100 nm semiconductor devices. Converging beam electron diffraction (CBED) in transmission electron microscopy (TEM) can be used to characterize the strain with nanometer-scale resolution [39,40]. But destructive and complicated sample preparations (which may alter the original strain field) have made this technique undesirable for large-scale strain characterization. Hence, reliable non-destructive quantitative assessment of strain in nanometer scale is critical. However, there is no such characterization technique available in the market. Here we show the strain measurement on the 65 nm device lines with much improved repeatability and excellent S/N ratio.

#92247 - $15.00 USD Received 29 Jan 2008; revised 2 Mar 2008; accepted 25 Mar 2008; published 19 May 2008

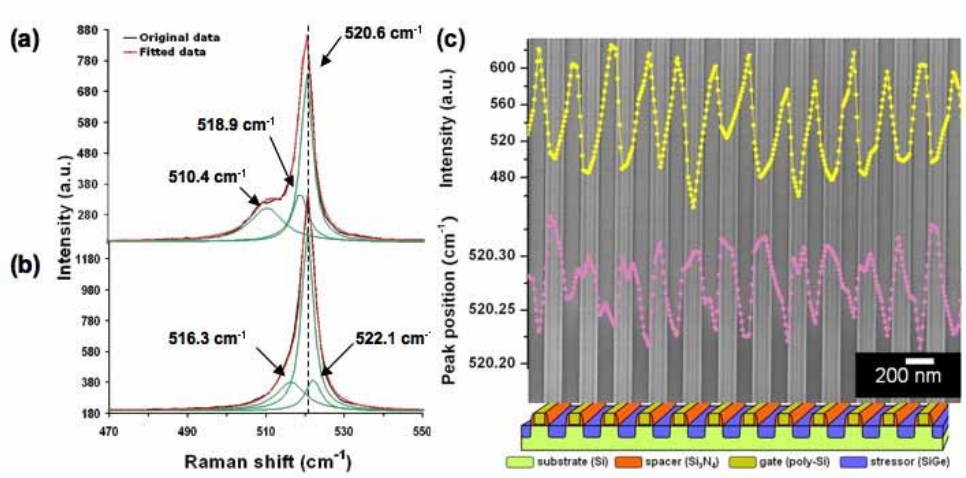

Fig. 2. The Raman spectra from (a) SiGe and (b) poly-Si lines with fitted peaks using Lorentzian function. In spectrum a, the Raman peak at 510.4 cm^{-1} corresponds to Si-Si phonon vibrations from SiGe, while the peaks at 518.9 and 520.6 cm^{-1} belong to tensile-strained Si just below the SiGe and the bulk Si substrate, respectively. In spectrum b, the Raman peaks at 516.3, 520.6 and 522.1 cm^{-1} correspond to Si-Si phonon vibrations of poly-Si, bulk Si substrate and compressively strained Si in the channel region, respectively. (c) Scanning Electron micrograph with cross-section view diagram of periodic poly-Si lines and SiGe stressors. Line-scan of Raman Si-Si intensity from SiGe is shown in yellow color, and the Si-Si peak position from the bulk Si is in purple color. The line scans show excellent correspondence with the structure.

Figures 2(a) and 2(b) show the Raman spectra recorded in the SiGe line region and on top of the poly-Si line, respectively. Each spectrum was fitted with three Lorentzian peaks. In Fig. 2(a), the Raman peaks from SiGe line correspond to Si-Si phonon vibrations from the SiGe (510.4 cm^{-1}), tensile-strained Si just below the SiGe (518.9 cm^{-1}), and the Si substrate below (520.6 cm^{-1}), respectively. Similarly, in Fig. 2(b), the Raman peaks correspond to Si-Si phonon vibrations of poly-Si (516.3 cm^{-1}) and bulk Si below (520.6 cm^{-1}), and another one is from compressively strained Si in the channel region (522.1 cm^{-1}).

Figure 2(c) shows the SEM image of the device sample together with the detailed illustration diagram of the device structure. From Fig. 2(c) we can see the line profile of the integrated intensity of Si-Si phonon vibrations from the SiGe (yellow color), and the Si-Si peak position from the bulk Si (purple color). The results show excellent correspondence with the device structure with good S/N ratio**.** The line profile data (intensity and peak positions) are extracted from an area Raman mapping of 4.0x1.3 μm^2 (100x32 points) shown in Fig. 3(c), which took about six minutes to complete.

#92247 - $15.00 USD Received 29 Jan 2008; revised 2 Mar 2008; accepted 25 Mar 2008; published 19 May 2008

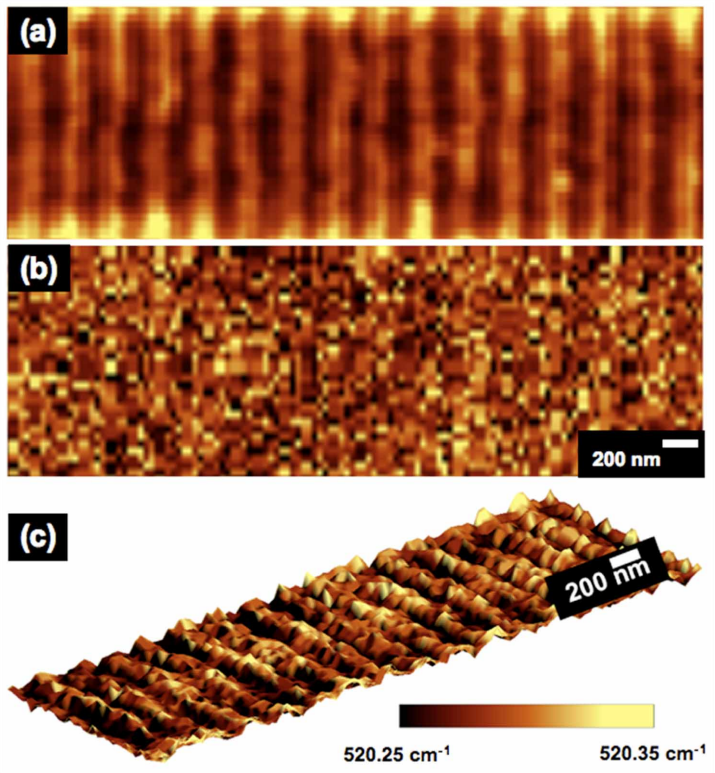

Fig. 3. (a) and (b) are 4.0x1.3 μm^2 near-field and confocal Raman images of the periodic poly-Si lines and SiGe stressors obtained in about six minutes, respectively, generated from the Si-Si peak intensity from SiGe. (c) 3D near-field Raman image from Si-Si peak position showing the relative strain at different regions.

Figures 3(a) shows the Raman image from the intensity of Si-Si phonon vibrations from the SiGe of the structure shown in Fig. 2(c). For comparison, Fig. 3(b) shows the image from confocal Raman setup (far-field imaging). It is clear that our near-field technique can resolve the periodic lines with excellent repeatability, but far-field technique cannot resolve the lines. The 3D near-field Raman image from Si-Si peak position at Fig. 3(c) was constructed from Gaussian fitting of the Si-Si phonon vibration. From this image we can study the higher compressive strain regions, which are under the poly-Si lines and compressively strained by the SiGe stressors. The fact that it took only about six minutes to carry out the mapping means high-resolution Raman imaging using our technique can be performed in reasonable time.

We have also performed Raman mapping on gold nanopatterns. Gold nanopatterns were fabricated on silicon substrate. Polystyrene microspheres of diameter 0.5 μm were purchased from Polysciences, Inc. The colloids were used as received and mixed with high purity de-ionized water to a density of approximately 10^{10} beads/ml. 20 μl of this solution were drop-coated on Si substrate. The polystyrene microspheres will self-assemble to form monolayer after drying. Gold thin film with a thickness of ~100 nm was deposited onto the Si substrate by using DC magnetron sputtering. The sample was sonicated for one minute in chloroform to remove the polystyrene microspheres. The sample was then annealed in Argon ambient at 400 ^{0}C for 30 minutes. The size of the gold nanopatterns is ~100 nm.

#92247 - $15.00 USD Received 29 Jan 2008; revised 2 Mar 2008; accepted 25 Mar 2008; published 19 May 2008

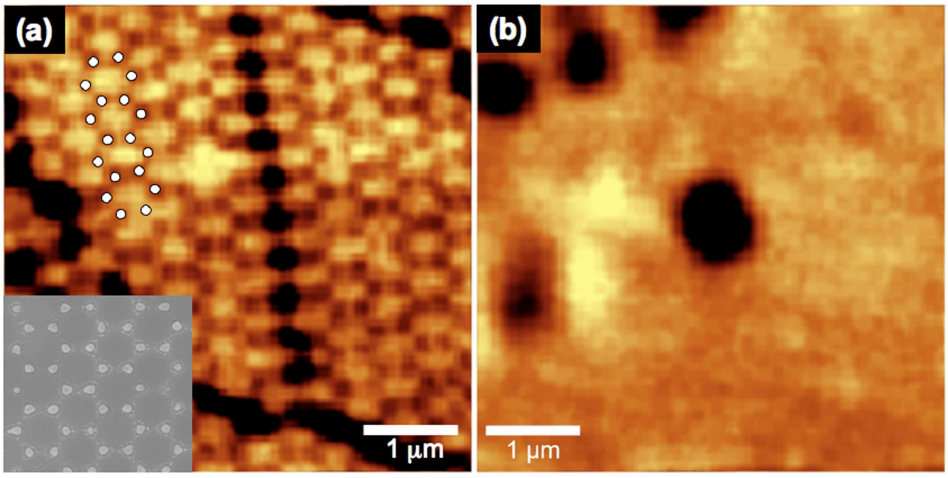

Fig. 4. (a) and (b) are 5.0x5.0 μm^2 near-field and confocal Raman images of the gold nanopatterns, respectively, generated using Si Raman peak intensity from the substrate. The white dots illustrate the gold nanopatterns on the substrate. Inset shows the SEM image of the gold nanopatterns with the size of the nanopatterns is ~100 nm.

Figures 4(a) and 4(b) show the 5.0x5.0 μm^2 (100x100 points) near-field and confocal Raman images of gold nanopatterns, respectively. Figure 4(a) shows the Raman image from the Si-Si peak intensity. Darker regions correspond to the gold nanopatterns. It can be clearly seen that the gold nanopatterns with the size of ~100 nm can be clearly resolved using our technique. The near-field Raman image corresponds well to the electron micrograph as shown in the inset of Fig. 4(a). The confocal Raman image of the gold nanopatterns shows no details of the patterns, as shown in Fig. 4(b). This proves the capability of our technique to various samples. Besides this, the spatial resolution can be improved further by reducing the Brownian motion of the microsphere in the solution, e.g. in sugar solution. We have achieved a spatial resolution (FWHM) of 48 nm by scanning the microsphere in 10% sugar solution (by weight). Adding too much sugar makes the solution too viscous and scanning becomes difficult. Smaller sizes of PS microspheres (0.5 μm and 1 μm) have also been used. However, the small dimension and Brownian motion have made the trapping difficult.

It is also important to note that the peaks from PS microsphere are not a big concern. For the study of Si device, the peaks from Si and PS are not at the same positions and the peaks from PS are generally weaker. However, this technique is not limited to the use of PS microsphere. Different types of dielectric microsphere can be used, e.g. SiO_2, TiO_2, ZrO_2 and so on. SiO_2 microsphere has the advantage of not giving any Raman peak. Besides this, higher resolution can even be achieved with the use of higher refractive index dielectric microsphere.

4. Conclusion

In conclusion, we report a new design in performing high-resolution near-field Raman imaging. High-resolution Raman image of PMOS transistors with SiGe source drain stressors was obtained by scanning a 3 μm diameter polystyrene microsphere using optical tweezers mechanism. The microsphere is used to focus the excitation laser, and also to collect the scattered Raman signal. The major advantages of this technique are non-destructive, high reproducibility (almost 100%), fast (strong signal), no far-field background, and easy to use compared to other near-field Raman techniques, e.g aperture and apertureless methods. We also showed the capability of this technique in studying the strain on sub-100 nm semiconductor device, in which Si channel is compressively strained by SiGe stressors. Besides on the device sample, high-resolution Raman imaging was also performed on gold nanopatterns on Si substrates. Although spatial resolution of this method (80 nm) is far from what has been achieved by TERS (10 nm), the spatial resolution can be improved further by

#92247 - $15.00 USD Received 29 Jan 2008; revised 2 Mar 2008; accepted 25 Mar 2008; published 19 May 2008

reducing the Brownian motion of the microsphere, e.g. by scanning the microsphere in sugar solution. Preliminary result has shown resolution of 48 nm can be achieved. Microsphere with higher refractive index, e.g. TiO_2, ZrO_2 microspheres also can be used to achieve better resolution. The simplicity and reproducibility of this approach to achieve high resolution Raman imaging will make it attractive to be used for large-scale applications in nano-science and nano-technology.

Acknowledgments

The authors would like to thank Nanyang Technological University and Chartered Semiconductor Manufacturing for the financial support.

#92247 - $15.00 USD Received 29 Jan 2008; revised 2 Mar 2008; accepted 25 Mar 2008; published 19 May 2008